2009

Unified theory of gas damping of flexible microcantilevers at low ambient pressures

Rahul A. Bidkar

Ryan C. Tung

Alina A. Alexeenko
Purdue University - Main Campus, alexeenk@purdue.edu

Hartono Sumali

Arvind Raman
Purdue University, raman@purdue.edu

Rahul A. Bidkar, Ryan C. Tung, Alina A. Alexeenko, Hartono Sumali, and Arvind Raman

Unified theory of gas damping of flexible microcantilevers at low ambient pressures

Rahul A. Bidkar,[1] Ryan C. Tung,[1] Alina A. Alexeenko,[2] Hartono Sumali,[3] and Arvind Raman[1,a)]

[1]*Birck Nanotechnology Center and School of Mechanical Engineering, Purdue University, West Lafayette, Indiana 47907, USA*
[2]*School of Aeronautics and Astronautics, Purdue University, West Lafayette, Indiana 47907, USA*
[3]*Sandia National Laboratories, Albuquerque, New Mexico 87185, USA*

Predicting the gas damping of microcantilevers oscillating in different vibration modes in unbounded gas at low pressures is relevant for increasing the sensitivity of microcantilever-based sensors. While existing free-molecular theories are valid only at very high Knudsen numbers, continuum models are valid only at very low Knudsen numbers. We solve the quasisteady Boltzmann equation and compute a closed-form fit for gas damping of rectangular microcantilevers that is valid over four orders of magnitude of Knudsen numbers spanning the free-molecular, the transition, and the low pressure slip flow regimes. Experiments are performed using silicon microcantilevers under controlled pressures to validate the theory. © *2009 American Institute of Physics*. [DOI: 10.1063/1.3122933]

This article focuses on the gas damping of long, slender vibrating microcantilevers immersed in an unbounded gas from atmospheric pressures down to ultrahigh vacuum. Such microcantilevers and microbeams are commonly used as pressure sensors,[1] biological mass sensors,[2] thermal and humidity sensors, radio-frequency switches and filters,[3] and atomic force microscopes, where gas damping prediction can enable a better system design. A relevant nondimensional parameter that governs the gas damping in these applications is the Knudsen number (Kn), the ratio of the mean free path of gas molecules to a characteristic dimension of the microcantilever. While viscous models[4,5] predict gas damping in the continuum and slip-flow regimes (for $Kn < 0.1$), free-molecular gas damping models[1,6] are valid only at near-vacuum pressures in the free-molecular regime (for $Kn > 10$) and break down at intermediate ambient pressures in the transition regime (for $0.1 < Kn < 10$). Clearly, a unified theory to accurately predict the gas damping of microcantilevers over different flow regimes would be very desirable.[7] In this work, we develop a Boltzmann equation based semi-analytical model to predict the gas damping of rectangular microcantilevers oscillating in the free-molecular, the transition and even the low pressure slip-flow regimes and validate the approach with detailed experimental results.

We begin with an analytical expression for gas damping in the free-molecular regime and discuss its limitation. Using the expression for drag force on a thin plate[8] in the free-molecular regime, the correct expression for gas force $F_d(x,t)$ per unit length of a rectangular microcantilever [see Fig. 1(a)] of width $2b$ moving with velocity $\dot{w}(x,t)$ along the z-direction is[8]

$$F_d(x,t) = c_f \dot{w}(x,t) = 2pb\left(2 - \sigma_v + \frac{\pi}{4}\sigma_v\right)\sqrt{\frac{8m}{\pi k_B T}}\dot{w}(x,t), \quad (1)$$

where c_f is the gas damping coefficient, p is the ambient pressure, σ_v is the momentum accommodation coefficient

and $\sigma_v = 1$ corresponds to the diffuse reflection case, m is the average mass of a gas molecule, k_B is the Boltzmann constant, and T is the absolute temperature. Equation (1) is valid only when pressures are low enough ($Kn > 10$) so that the collisions between gas molecules are negligible and only the gas-microcantilever collisions are important.

In order to develop a gas damping model that is uniformly valid over four orders of magnitude of ambient pressure ($10^3 < Kn < 0.1$), we assume that the microcantilever (see Fig. 1) is long compared to its width so that the gas flow calculations are restricted to a cross-section parallel to the yz-plane. The gas flow in this two-dimensional domain is governed by the quasisteady Boltzmann equation[8,9]

$$V\frac{\partial f}{\partial y} + W\frac{\partial f}{\partial z} = \nu(f_o - f), \quad (2)$$

where $f(y,z,\mathbf{u})$ is the distribution function, y and z are the Cartesian coordinates, $\mathbf{u} = U\mathbf{i} + V\mathbf{j} + W\mathbf{k}$ are the gas velocities along the Cartesian coordinates, and ν is the collision frequency. The ellipsoidal statistical Bhatnagar–Gross–Krook (ES-BGK) collision operator[9] on the right side of Eq. (2) is[9]
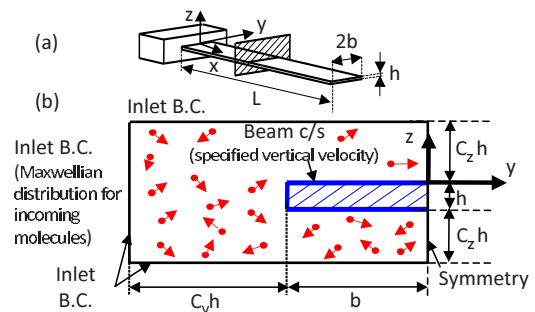

FIG. 1. (Color online) (a) A schematic of the microcantilever with length L, width $2b$ and thickness h, and (b) a schematic representation of the boundary conditions for the ES-BGK calculations imposed in the computational model (cantilever cross-sectional plane).

a)Electronic mail: raman@ecn.purdue.edu.

$$f_o(y,z,\mathbf{u}) = \frac{n(y,z)}{\sqrt{(2\pi)^3 \det[\Lambda_{ij}]}} \exp\left(-\frac{\epsilon_{ij}}{2} c_i c_j\right), \qquad (3)$$

where $\Lambda_{ij} = RT\delta_{ij}/Pr + (1-1/Pr)p_{ij}/\rho_f$, $i,j=1,2,3$, $n(y,z)$ is the number density, $\mathbf{c}=\mathbf{u}-\overline{\mathbf{u}}$ is the thermal velocity of gas molecules, $\overline{\mathbf{u}}$ is the average velocity of the gas molecules, R is the gas constant, $[\epsilon]=[\Lambda]^{-1}$, $p_{ij}(y,z)$ is the pressure tensor, $\rho_f(y,z)$ is the mass density of the gas, $Pr=\mu c_p/K$ is the Prandtl number, μ is the dynamic viscosity, c_p is the specific heat at constant pressure, and K is the thermal conductivity.

Equations (2) and (3) are solved numerically using an in-house computer program.[9] The boundary conditions for the computational domain are shown in Fig. 1(b). The size of the computational domain, and the spatial and velocity grid resolution were chosen after rigorous convergence studies.[10]

The computed normal pressure $p_{33}(y)$ is integrated along the width of the beam to obtain the gas force $F_d(x,t)$ per unit length of the microcantilever for beam aspect ratios $\kappa = 2b/h = 10$, 20, 35, and 50 and Kn numbers varying from $1/\kappa$ to $(3.2\times10^4)/\kappa$. The Kn numbers used in the computations are calculated using $Kn = k_B T/(\sqrt{2}\pi d^2 pb)$, where d is the diameter of gas molecules.

Based on these computations, we present a closed-form fit for the gas force $F_d(x,t) = c_f \dot{w}(x,t)$, where the gas damping coefficient c_f is expressed in terms of two nondimensional numbers $\gamma = \log_{10}(\kappa)$ and $\tau = \log_{10}(Kn\ \kappa/2)$:

$$\log_{10} c_f(\gamma,\tau) = \log_{10}\left(2pb\sqrt{\frac{8m}{\pi k_B T}}\right)$$
$$+ \frac{[(0.1392\gamma+0.4569)\tau^4 + (0.2251\gamma-0.0039)\tau^3 + (-0.7089\gamma+1.9703)\tau^2 + (-0.4225\gamma+1.2943)\tau - 2.559\gamma+1.3292]}{[(0.7862\gamma+1.6159)\tau^4 + (-0.9158\gamma+2.0428)\tau^3 + (0.0348\gamma+2.636)\tau^2 + (-1.9568\gamma+6.8491)\tau + 1.0398\gamma+2.9195]}. \qquad (4)$$

The maximum error between the computed values and the fit for c_f over the entire data range was less than 1.8%. The correlation in Eq. (4) is valid for diffuse reflection of gas molecules from rough surfaces of microcantilevers with aspect ratios $\kappa = 2b/h$ ranging from 10 to 50 oscillating in any diatomic gas at any ambient temperature and pressure as long as the Kn number is larger than $1/\kappa$.

The closed-form fit Eq. (4) can be conveniently used to predict the damping ratio $\zeta_{gas,n}$ or Q-factor ($Q_{gas,n}$) of a microcantilever (with or without a tip mass) oscillating in an unbounded gaseous medium in its nth vibration mode as follows:

$$\zeta_{gas,n} = \frac{c_f(\gamma,\tau)}{2\rho_c A_c \omega_n}, \qquad Q_{gas,n} = \frac{\rho_c A_c \omega_n}{c_f(\gamma,\tau)}, \qquad (5)$$

where ρ_c is the structural density, $A_c = 2bh$, and ω_n is the nth natural frequency of the microcantilever that can be computed analytically using thin beam theory.[11]

In order to validate the model predictions, detailed experiments were performed in a MMR vacuum probe station (MMR Technologies) at the Sandia National Laboratories (SNL), New Mexico using five phosphorus-doped silicon microcantilevers with different characteristic frequencies (CSC12/tipless probes A, B, C, E, and F from MikroMasch, Inc.;[12] see Table I). The microcantilevers were inertially excited by mounting the microcantilever chip on dither piezo. The vibration mode shape and the frequency response functions (FRFs) of 30 grid points, i.e., the ratio of the velocity of a point on the microcantilever to the velocity of the base of the microcantilever were measured with a scanning laser-doppler vibrometer (MSA400 from Polytec, Inc.). The experimental data presented in this work are averaged over ten repeated sets of data at each value of ambient pressure. Data were collected at 19 equally spaced air pressures on the $\log_{10}$ scale from 83 593 to 0.133 Pa. For pressures larger than 100 Pa, the total damping ratio ζ was estimated from the experimental FRFs,[13] while for lower pressures, ζ was estimated

from the envelope of the freely decaying motion of the microcantilevers.[13] Finally, the structural damping ζ_{struc} is systematically extracted[14] and then subtracted from ζ to obtain the gas damping ζ_{gas}.

A comparison of the predicted and the measured gas damping ratios for microcantilevers A, C, and F oscillating in the fundamental and higher modes is shown in Fig. 2. For pressures between 10 Pa($Kn=30.6902$) and 2700 Pa($Kn=0.1137$), the rms error was less than 7% for microcantilevers A and C, and the rms error was less than 20% for microcantilever F; microcantilevers B and E presented noisier data and are not presented here. The quasisteady ES-BGK model predicts gas damping for intermediate pressures where both the free-molecular model[8] and the continuum regime theories (the no-slip unsteady Stokes model[4]) fail to capture the transition from one regime to another. The predictions of the fit in Eq. (4) also agree with the experimental data of Bianco *et al.*[15] (rms error less than 12% for pressures between 3 Pa($Kn=35.805$) and 600 Pa($Kn=0.1790$)) for a microcantilever with nominal $h=5$ μm and nominal $\kappa=20$.

The predictions of the current theory diverge from the measured gas damping values for pressures lower than

TABLE I. Geometric properties and frequencies of phosphorus-doped silicon microcantilevers (Ref. 12) with $\rho_c = 2330$ kg/m^3 and Young's modulus $E=169$ GPa (Ref. 12). The length and the width are obtained from scanning electron microscope images of the microcantilevers. The thickness h is estimated by choosing h such that it minimizes the rms error between the predicted and measured *in vacuo* frequencies for the first three modes of each microcantilever.

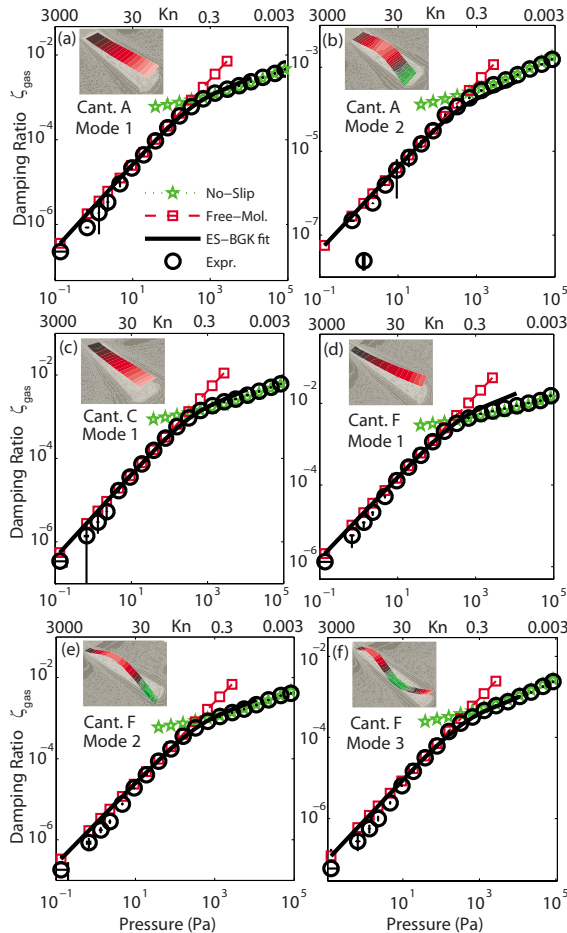| Quantity (units)	Cant. A	Cant. C	Cant. F
Length $L(\mu m)$	111	132	258
Width $2b(\mu m)$	32	32.5	31
Thickness $h(\mu m)$	1.050	1.003	1.003
Freq. 1 (KHz)	114.415	75.183	19.085
Freq. 2 (KHz)	763.780	502.860	134.120
Freq. 3 (KHz)	⋯	1462.750	388.270

FIG. 2. (Color online) Comparison of the predictions of the free-molecular model (Ref. 8), the no-slip unsteady Stokes flow model (Ref. 4) and the ES-BGK-model-based fit with the experimental gas damping values for microcantilever (a) A in its first mode, (b) A in its second mode, (c) C in its first mode, (d) F in its first mode, (e) F in its second mode, and (f) F in its third mode. The horizontal bars on the experimental values are due to the uncertainty in pressure values and the vertical bars represent the uncertainty caused due to the uncertainty in estimating structural damping. The insets are the experimentally measured vibration modes.

FIG. 3. (Color online) The normalized pressure p^* and the stream-traces plotted for (a) $Kn=3$ and (b) $Kn=0.03$. Note that only half width of the microcantilever is shown for each of the two cases.

numbers, the gas molecules collide over much shorter length scales and the shearing of fluid near the microcantilever edges, in the form of stream-traces turning back over smaller length scales, becomes a dominant feature of the surrounding gas flow [see Fig. 3(b)]. This transition in flow physics cannot be handled by either the free-molecular[8] or the no-slip Sader[4] model alone.

In summary, we have developed and validated a closed form fit for the gas damping of microcantilevers as a function of the Kn number and the aspect ratio κ of the beam cross section. The theory is valid for long, rectangular cross-section microcantilevers oscillating in the free-molecular, transition, and low-pressure slip regimes in arbitrary vibration modes, at any temperature and in any diatomic gas.

10 Pa ($Kn > 30.6902$) and pressures higher than 2700 Pa ($Kn < 0.1137$). The disagreement at pressures lower than 10 Pa could be because the theoretical model assumes unbounded gas whereas in experiments, the surrounding gas is bounded because the mean free path of the gas is comparable to the gap between the microcantilever and the substrate. The discrepancy at higher pressures ($p > 2700$ Pa) occurs because the current model neglects the unsteady gas inertia term. An unsteady Boltzmann equation model[8,16] or a continuum regime slip-flow model[5] is expected to work better for such high pressures.

Both the theory and experiments clearly show that the gas damping displays markedly different slopes for high Kn and low Kn numbers. To understand the physics underlying these differences, we consider the computed stream-traces emanating from the microcantilever surface and the pressure field $p^*=(p-p_{ambient})/p_{ambient}$, for two different Kn numbers 3 and 0.03. For the case of $Kn=3$ [see Fig. 3(a)], a *uniform* pressure acts along the entire width of the beam because in a low intermolecular collision flow, gas molecules are equally likely to exchange momentum with all locations along the width of the beam. On the other hand, for very small Kn
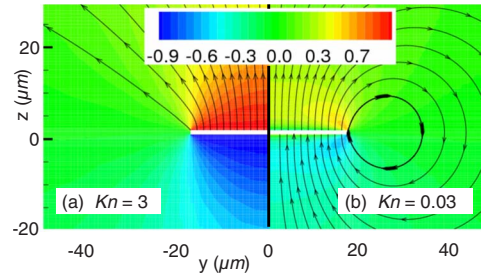
[1] F. R. Blom, S. Bouwstra, M. Elwenspoek, and J. H. J. Fluitman, J. Vac. Sci. Technol. B **10**, 19 (1992).
[2] P. S. Waggoner and H. G. Craighead, Lab Chip **7**, 1238 (2007).
[3] L. Liwei, R. T. Howe, and A. P. Pisano, J. Microelectromech. Syst. **7**, 286 (1998).
[4] J. E. Sader, J. Appl. Phys. **84**, 64 (1998).
[5] M. J. Martin and B. H. Houston, AIAA-2008-690.
[6] R. G. Christian, Vacuum **16**, 175 (1966).
[7] K. Kokubun, M. Hirata, M. Ono, H. Murakami, and Y. Toda, J. Vac. Sci. Technol. A **5**, 2450 (1987).
[8] T. I. Gombosi, *Gaskinetic Theory* (Cambridge University Press, New York, 1994).
[9] A. A. Alexeenko, S. F. Gimelshein, E. P. Muntz, and A. D. Ketsdever, Int. J. Therm. Sci. **45**, 1045 (2006).
[10] With domain size parameter $C_y=C_z=130$, and 225 by 332 grid points in the yz plane, the gas damping predictions converged within 2.5%.
[11] S. S. Rao, *Mechanical Vibrations* (Pearson Prentice Hall, New Jersey, 2004).
[12] Mikromasch, Inc., San Jose, CA, USA, http://www.spmtips.com.
[13] H. Sumali, J. Micromech. Microeng. **17**, 2231 (2007).
[14] Structural damping ratio ζ_{struc} is estimated by linearly extrapolating to zero absolute pressure the measured damping trend at the lowest three pressures (0.133, 0.665, and 1.33 Pa), where the gas flow is truly free-molecular, thereby allowing us to assume a linear dependence of gas damping on the ambient pressure (Refs. 6 and 8).
[15] S. Bianco, M. Cocuzza, S. Ferrero, E. Giuri, G. Piacenza, C. F. Pirri, A. Ricci, L. Scaltrito, D. Bich, A. Merialdo, P. Schina, and R. Correale, J. Vac. Sci. Technol. B **24**, 1803 (2006).
[16] S. Chigullapalli, A. Venkattraman, and A. A. Alexeenko, AIAA-2009-1317.